Photodiagnosis and Photodynamic Therapy 51 (2025) 104440

Contents lists available at ScienceDirect

Photodiagnosis and Photodynamic Therapy

journal homepage: www.elsevier.com/locate/pdpdt

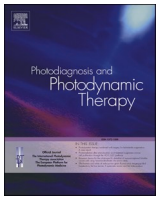

Proposal and operational evaluation of a device for external and internal photodynamic therapy treatments

Enrique Navarrete de Gálvez [a,*], Pablo Fonda Pascual [b], José Aguilera Arjona [c], José Ramón de Andrés Díaz [a], María Navarrete de Gálvez [d], Shiran Perera Mohamed [a], María Victoria de Gálvez Aranda [c]

[a] Project Engineering Area, Department of Graphic Expression Design and Projects, University of Málaga, Málaga, Spain
[b] Dermatology Department, Gómez Ulla Hospital Central de la Defensa, Madrid, Spain
[c] Photobiological Dermatology Laboratory Medical Research Centre, Department of Dermatology and Medicine, Faculty of Medicine, University of Málaga, Málaga, Spain
[d] Internal Medicine Service, Hospital Universitario Virgen de la Victoria, Málaga, Spain

ARTICLE INFO

Keywords:
Absorption spectrum
Emission spectrum
LED device
Photodynamic therapy (PDT)
Photosensitizer

ABSTRACT

Photodynamic therapy (PDT) light sources must match their emission spectrum with the absorption spectrum of the photosensitizer, provide precise treatment definition, deliver adequate irradiance, avoid thermal damage, and minimize treatment duration. Additionally, they should be adaptable to different photosensitizers, easy to manipulate, and cost-effective.

Current LED sources are difficult to customize, rigid, and primarily designed for broad-area treatments. For localized treatments, laser technology is commonly employed.

We propose a customizable and programmable LED-based device that not only meets these specifications but also addresses the limitations of current LED sources for localized treatments. It allows for the connection of a fiber optic terminal for internal treatments and can be fitted with light-diffusing devices capable of treating lesions externally or penetrating them internally. This device is an enhanced version of a previously developed source that has demonstrated efficacy in several pilot studies of photodynamic therapy.

The proposed equipment shows significant potential for both medical and research applications, enabling the configuration of emission spectra on demand and the establishment of tailored treatment protocols based on the type of lesion being treated.

1. Introduction

Photodynamic therapy (PDT) is a minimally invasive medical technique with minimal side effects (pain manageable with analgesics), no cumulative toxicity, and is approved for the treatment of various types of lesions, while also being studied for additional applications. Among these lesions are actinic keratosis, basal cell carcinoma, Bowen's disease, acne, rosacea, skin aging, esophageal cancer, Barrett's dysplasia, gastric cancer, and colorectal malignancies, among others [1,2].

An indirect photodynamic therapy treatment requires three elements: oxygen, a photosensitizing molecule (sometimes applied directly, sometimes induced by the supplied photosensitizer), and light [3–5]. Light serves as the activating element that initiates the sequence of chemical reactions described in the Jablonski diagram [3–8]. This process induces hyperoxidative stress, with the primary effect generally being the death of the target cell through a combination of necrosis and apoptosis. Indirect effects that promote the elimination of treated lesions also exist [9].

Not all infrared radiation, visible light, and ultraviolet radiation can activate the Jablonski reaction; only those wavelengths that correspond to the sensitivity ranges of the photosensitizing molecule can do so. In dermatology, precursors of protoporphyrin IX (PpIX) are predominantly employed. This photosensitizing molecule has five activation bands: 409 nm (Soret band), and 509, 544, 548, and 634 nm (Q bands) [4,10–12]. In addition to PpIX precursors, there are also porphyrins, porphycenes, phthalocyanines, chlorins, pheophorbides, Bengal rose, methylene blue, and others. Each of these is characterized by a specific absorption spectrum [7,13].

* Corresponding author at: Project Engineering Area, Department of Graphic Expression Design and Projects, School of Industrial Engineering, University of Málaga, Málaga, Campus Universitario de Teatinos S/N, 29071-Málaga, Spain.
E-mail address: endg@uma.es (E. Navarrete de Gálvez).

https://doi.org/10.1016/j.pdpdt.2024.104440
Received 5 November 2024; Received in revised form 25 November 2024; Accepted 4 December 2024
Available online 5 December 2024

When selecting a light source to excite the photosensitizing molecule, it is essential first to analyze the correspondence between the emission spectrum of the source and the absorption spectrum of the photosensitizing molecule. It is also necessary to consider treatment duration, lesion depth, lesion location (external/internal), lesion size, and operator training in the use of the equipment, among other variables.

The development of personalized light delivery devices capable of meeting the aforementioned requirements could significantly impact the enhancement of this technique and expand its range of applications.

Traditionally, photodynamic therapy has utilized laser sources [14] for superficial lesions, due to the limited penetration capacity of radiation in tissues. Laser sources have high irradiance, which reduces treatment times, and they can be used through direct irradiation or coupled to optical fibers, allowing for internal treatments via endoscopy. However, aside from their high costs, challenges include maintenance, the need for qualified personnel for operation, recalibrations, and technical support.

As an alternative to laser sources, lamps for photodynamic therapy have been developed—more economical devices featuring simpler, portable designs that require less maintenance and are easier to use. These emitters possess a broad spectrum, which allows for the excitation of the photosensitizer at several of its absorption peaks; however, this comes with the associated disadvantage that achieving specific spectra requires filters, leading to losses and complicating the determination of effective doses. The first lamps for photodynamic therapy were developed for treating large surfaces, making the use of optical fibers to direct radiation to well-defined or internal lesions complex [14].

In this line of research, there are proposals ranging from earlier designs, such as a prototype of a short-arc plasma discharge lamp with a filter to achieve an emission spectrum of 630 ± 15 nm, tested in actinic keratosis and Bowen's disease with a high cure rate [15], to more modern approaches, such as light-emitting fabrics developed by integrating flexible optical fiber emitters into textiles [16].

Currently, external and superficial lesions (1 to 2 mm in depth) are being treated with PpIX-inducing photosensitizers and with high success rates. For the treatment of internal lesions and those thicker than 1 cm, proposals requiring optical fiber conductors fitted with a directional diffusing tip or equivalent systems capable of penetrating the lesion focus and administering a specific dose of light from within are available [17,18].

These new proposals necessitate the design of sources that can accommodate optical fiber terminals to conduct light from the emitter to the light-diffusing terminal at the end of the fiber, which will be positioned to irradiate the lesion being treated, whether superficially or internally.

Considering the potential of photodynamic therapy for new treatments against significant diseases such as cancer and other types of lesions [18], this contribution presents a source based on LED technology, featuring a configurable and adjustable spectrum tailored to the requirements of the utilized photosensitizer, capable of accommodating an optical fiber terminal, with sufficient irradiance to compensate for losses in the optical fiber and achieve fluences at the terminal diffuser ranging from 100 to 300 mW/cm^2 [5] (irradiances exceeding 150 mW/cm^2 are not recommended to prevent thermal damage [19]). This source is characterized by being economical, requiring minimal maintenance, easy to use, and capable of delivering localized treatments.

The development of this device builds on a previously patented design, tested in a pilot study, with promising results [20] in skin lesions (see Fig. 1) and the treatment of onychomycosis (see Fig. 2).

The proposed device consists of a hollow, approximately cylindrical main body, about 15 cm in length and 4 cm in diameter, 3D-printed in insulating plastic material, which serves as a grip for the assembly and as a passage for the wiring. An aluminum piece is developed into 6 arms arranged at 60° intervals, each with three inclined planes at an angle of 160°. On each of the three inclined planes of each arm, a printed circuit board, LED diode (each arm with a different wavelength: 405–480–530–630–660–780 nm), and focusing lens are placed. The printed circuits are connected in series by wavelength, forming six LED matrices, one per arm, which are powered by six different constant current sources to allow independent control by wavelength. This aluminum piece is secured by a through screw and corresponding nut to the lower part of the main body. The assembly composed of the aluminum piece and the components installed on it is enclosed by hemispherical deflectors 3D-printed in plastic material, also fixed to the central body via a through screw. The geometric configuration of the aluminum piece supporting the LEDs, combined with the use of focusing lenses placed over each diode, allows the light to be focused on a treatment surface of approximately 0.2 cm^2, corresponding to a circle about 0.5 cm in diameter. The lower deflector has a central threaded opening to which a 3D-printed plastic terminal can be attached for an optical fiber cable or simply used as an outlet for the treatment light. Each of the power sources supplying the LED matrices is controlled by a 0/10 V PWM Bluetooth device, which receives commands for power on/off, timing, intensity, etc., from the digital device. These components end in a single connection cable to the power supply network. The power sources, Bluetooth PWM 0/10 V devices, and associated wiring are housed in a purpose-designed box, 3D-printed in plastic material. This box will feature a compartment on the top, accessible to the operator, for the placement of the digital equipment that controls the Bluetooth PWM 0/10 V devices. The box also includes a general power on/off button, fuse, and female connector to which the male connector of the cable leading to the distribution network will be connected (see Fig. 3).

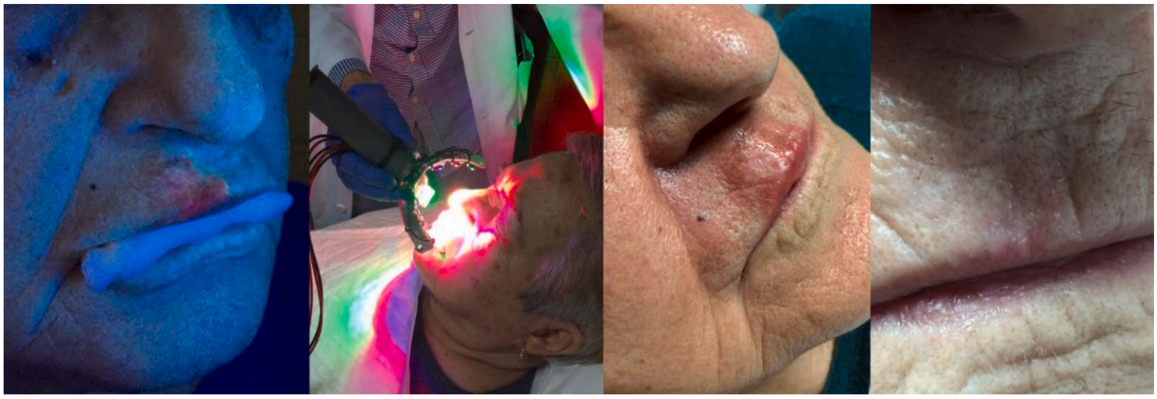

Fig. 1. Example of treatment for actinic cheilitis and results using the previously patented device [20].

Fig. 2. Example of onychomycosis treatment and results with previously patented device.

Fig. 3. Image of version 2.0 of the proposed device assembly.

2. Materials and methods

The main features of the device design are shown in Fig. 4, which illustrates the key elements of the device, including the fiber optic coupling terminal.

An aluminum piece with 6 arms was designed using 2D CAD software (AutoCAD). The CAD file was used with a numerical control machine to cut the new piece, which was subsequently bent according to the design specifications.

The main body of the device, deflectors, connector for the fiber optic terminal, and component housing were designed using 3D CAD software for mechanical modeling (SolidWorks). All elements were printed in insulating plastic material (PLA) using a Qidi Tech I-Fast printer.

Each LED diode + lens mounted in the luminaire (405–480–530–630–660–780 nm) was independently characterized. For this, the LEDs were placed on a simple aluminum PCB with a pack for the diode, positive/negative power connections, and 2 fixing holes. To ensure proper measurement under working conditions, a PROMAX FAC-662B dual power source was used, setting the supply current to 350 mA. The measurements were performed in a dark laboratory after the current had stabilized. The distance between the emitter and the sensor was 6 cm in all cases. A laboratory clamp was used to position the emitter in front of the sensor (see Fig. 5a).

To determine the biological irradiance of the device without the fiber optic terminal attached, the prototype was mounted at a treatment distance of 6.25 cm. Independent measurements were taken for each wavelength: first, the violet matrix at 405 nm, then the cyan matrix at 480 nm, followed by the green matrix at 530 nm, the red matrix at 630 nm, the red matrix at 660 nm, and the far-red matrix at 780 nm. Finally, measurements were taken with all matrices operating simultaneously (see Fig. 5b).

To determine the biological irradiance of the device with the fiber optic terminal attached (access means for the treatment of internal lesions), the prototype was mounted at a treatment distance of 0.5 cm. Independent measurements were taken for each wavelength: first, the violet matrix at 405 nm, then the cyan matrix at 480 nm, followed by the green matrix at 530 nm, the red matrix at 630 nm, the red matrix at 660 nm, and the far-red matrix at 780 nm. Finally, measurements were taken with all matrices operating simultaneously (see Fig. 5c).

The installed fiber optic terminal is autoclavable, featuring a 4 mm active core diameter, silicone coating, a length of 1.8 m, and a Wolf-Storz type connection interface.

The spectral irradiance measurements were performed using a MACAM SR-2271 double monochromator spectroradiometer (Irradian Co., Scotland, UK), connected via an optical fiber to an Ulbricht-type integrating sphere sensor. The spectroradiometer was calibrated for both wavelength and irradiance at the National Optics Center, using a certified UV–Visible calibration lamp.

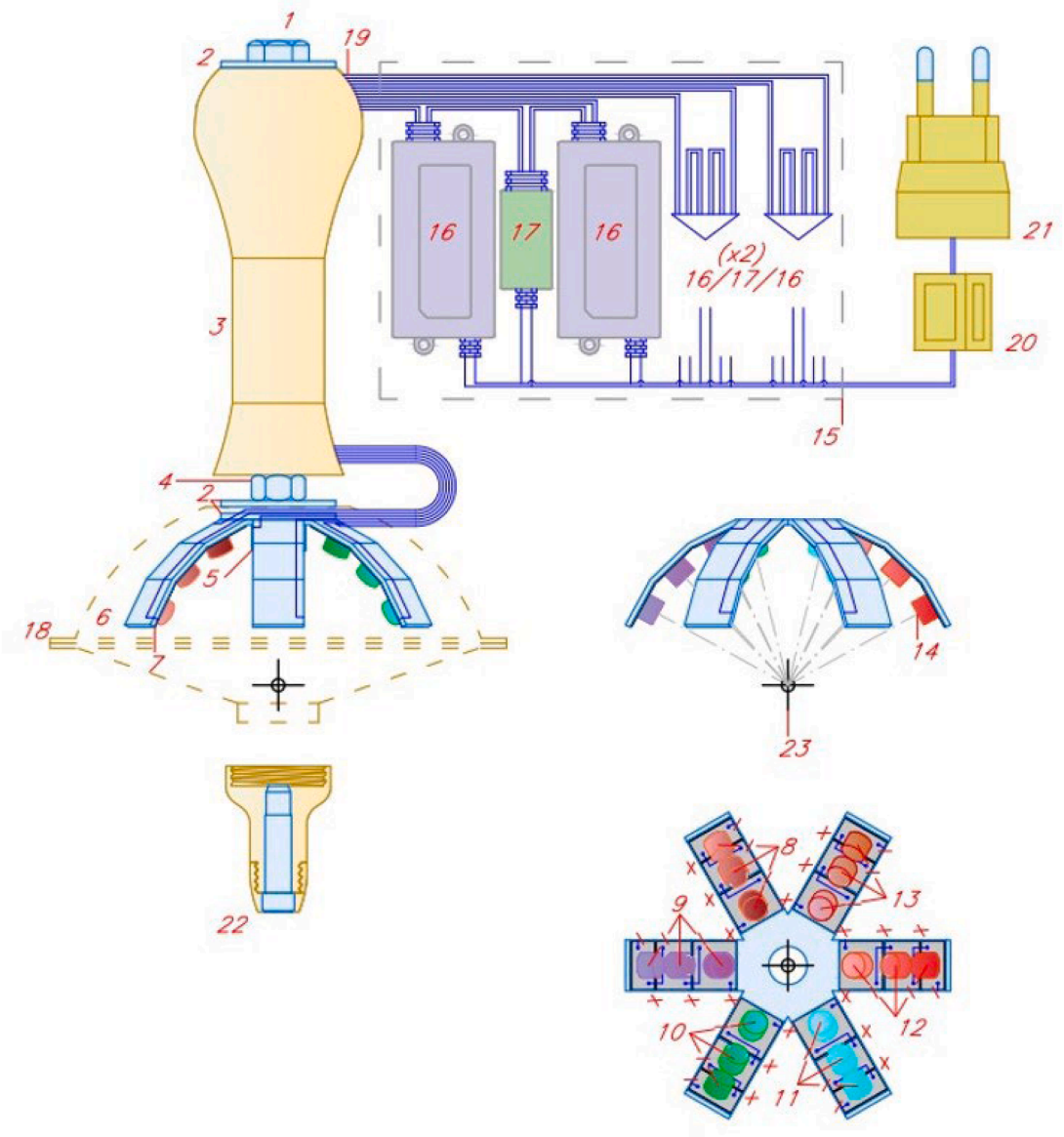

Fig. 4. Schematic representation of the proposed light source for photodynamic therapy. 1.-Assembly screw for the body with a six-arm aluminum body. 2.-Mounting washer. 3.-Arm printed with insulating plastic material (PLA). 4.-Positioning nut for the six-arm aluminum body. 5.-Self-locking nut for securing the assembly. 6.-Aluminum body with LED arrays arranged in six arms. Aluminum component with LED arrays arranged in three arms. 7.-Printed circuit board for mounting high-power LEDs. 8.-High-power LED with a peak wavelength of 632 nm. 9.-High-power LED with a peak wavelength of 407 nm. 10.-High-power LED with a peak wavelength of 518 nm. 11.-High-power LED with a peak wavelength of 474 nm. 12.-High-power LED with a peak wavelength of 634 nm. 13.-High-power LED with a peak wavelength of 783 nm. 14.-Concentrating lens. 15.-Body printed with insulating plastic material (PLA). 16.-LED matrix controller. 17.-Bluetooth PWM 0/10 V device with regulation capacity for two controllers. 18.-Semi-spherical enclosure for the aluminum body with LED arrays arranged in six arms, printed with insulating plastic material (PLA). 19.-DC power wiring for the LED assembly. 20.-On/off switch and fuse. 21.-Low-voltage mains plug (230 V 50 Hz). 22.-Terminal coupling piece for fiber optic endoscope to device. 23.-Light concentration point.

In each case, five measurements were taken. The mean spectral irradiance values were presented with a standard deviation, which in all cases was <2 %.

An analysis was carried out to evaluate the compatibility of our prototype with the use of different photosensitizers, some approved for medical use, others employed in research. For this purpose, the emission spectrum of our prototype was superimposed with the absorption spectra of some of the most commonly used photosensitizers in these types of therapies.

3. Results

The characterization of the LED + Lens setup at 6 cm yielded the results shown in Table 1 and Fig. 6.

The characterization of the assembled prototype at 6.25 cm, without the fiber optic terminal attached, yielded the results shown in Table 2 and Fig. 7a

The characterization of the assembled prototype, with the fiber optic terminal attached at 0.50 cm, yielded the results shown in Table 3 and Fig. 7b

The compatibility study between the proposed light source and the photosensitizers porphyrins, chlorins, bacteriochlorins, methylene blue, and rose bengal is presented in Fig. 8. It is observed that the equipment is optimized for treatments with PpIX precursors. However, it also exhibits good characteristics for use with other photosensitizers.

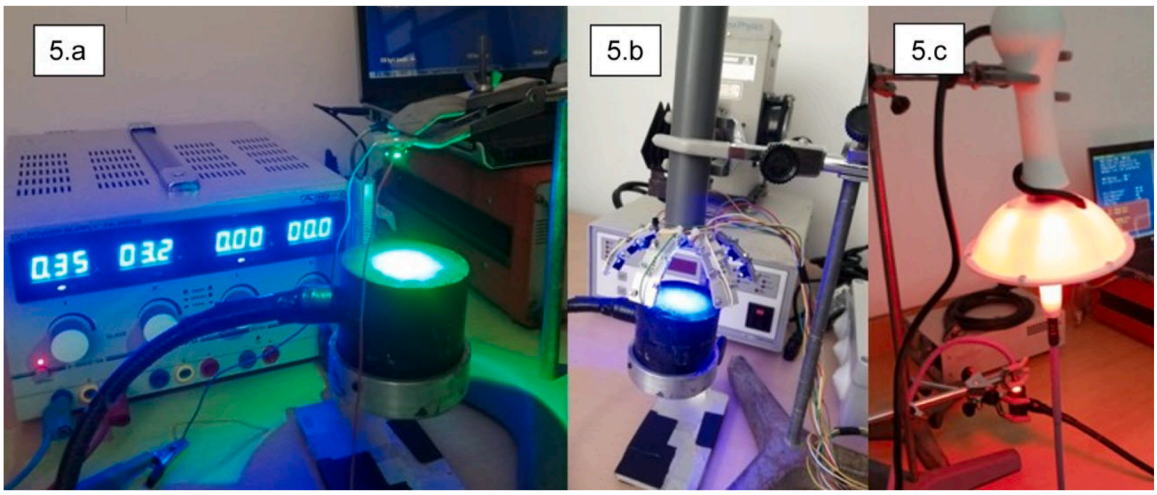

Fig. 5. a.- Characterization of the LED diode and lens prior to assembly in the device. b.- Characterization of the assembled device. c.- Characterization of the device with the endoscope terminal attached. In all cases, the source to be characterized is mounted at the treatment distance and directed into an Ulbricht integrating sphere, connected to a MACAM SR-2271 dual monochromator spectroradiometer (Irradian Co., Scotland, UK).

Table 1
Characterization of LED + Lens at 6 cm: spectrum peaks, spectral bandwidth at 50 % irradiance, emission spectrum symmetry, and absolute irradiance.

Color	Red	Red	Violet	Cyan	Infrared	Green
Peak [nm]	632	634	407	474	783	518
Spectral Bandwidth 50 % irradiance [nm]	627–637	628–640	402–412	465–483	776–790	507–529
Spectral Bandwidth symmetry	Symmetric	Symmetric	Symmetric	Asymmetric	Symmetric	Symmetric
Absolute Irradiance [mW/cm^2]	30.22	54.10	71.97	36.04	57.95	33.84

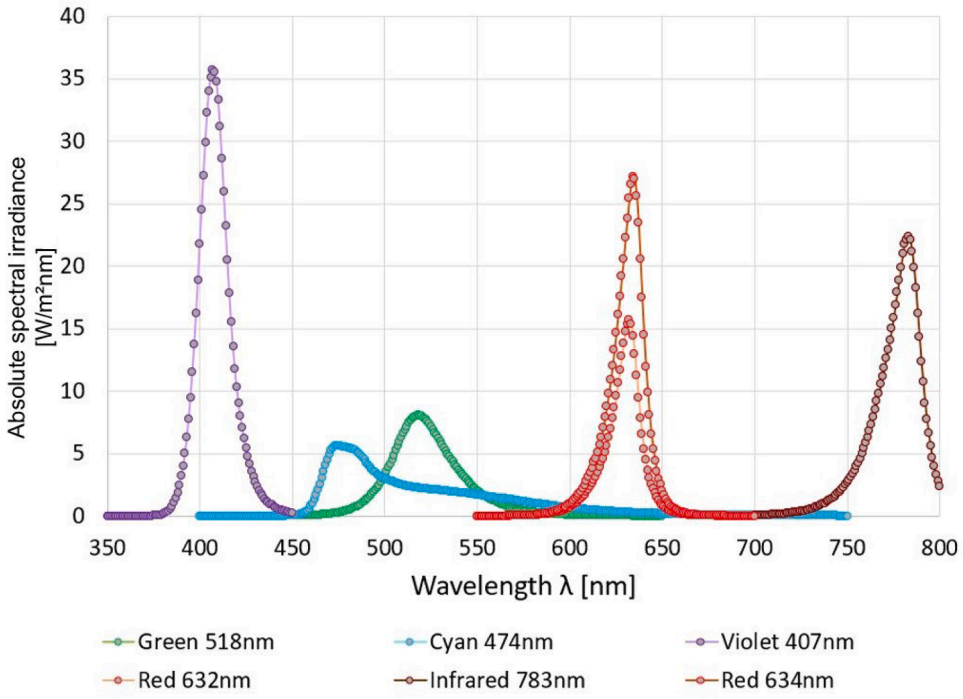

Fig. 6. Emission spectra of LEDs mounted on the device.

4. Discussion

The presented light source, in addition to the 3D-printed plastic enclosure, develops upon the previous patented and tested device by adding three additional arms with three additional wavelengths: red peak at 634 nm, cyan peak at 474 nm, and infrared peak at 783 nm. It also incorporates a Bluetooth PWM 0/10 V device for each pair of drivers (one per arm and wavelength). This device will receive commands for on/off, timing, intensity, etc., from a digital system. This new configuration allows for linear irradiance control per arm (compared to

Table 2
Characterization of assembled prototype without the fiber optic terminal attached at 6.25 cm: spectrum peaks, absolute irradiance for a 100 % PWM Cycle, and for a 50 % PWM cycle.

Color	Red	Red	Violet	Cyan	Infrared	Green
Peak [nm]	632	634	407	474	783	518
Absolute Irradiance [mW/cm²] PWM Cycle 100 %	93.27	127.03	130.91	160.29	123.75	89.79
Absolute Irradiance [mW/cm²] PWM Cycle 50 %	48.88	64.98	52.35	89.28	58.78	48.98

Note: 1.- The device with all LED arrays active, 691.37 (100 %)−342.53 (50 %) mW/cm². 2.- PWM Cycle 100 % The PWM delivers 100 % of the power to the end receivers. PWM Cycle 50 % The PWM delivers 50 % of the power to the end receivers.

the previous all-or-nothing system), enabling the programming of fixed or variable timing/irradiance duality for each arm independently, making it possible to create different treatment protocols tailored to various types of lesions. The option to attach a fiber optic endoscope terminal for internal treatments has also been added. This new configuration, which maintains a treatment area of 0.2 cm² (corresponding to a circle with a diameter of 0.5 cm), allows treatments with a high degree of precision on small surfaces and significantly increases the versatility of the device, whether for medical photodynamic therapy treatments or for research purposes.

The mounted LED emitters + lenses radiate sufficient energy to ensure, for external treatment (without the use of the endoscope terminal), irradiance adjusted by the action of several arms to 150 mW/cm², the maximum recommended value to avoid thermal damage, thus achieving the shortest treatment times. For internal treatments, we observe significant losses in the reception and transmission of light along the fiber optic endoscope terminal, with losses around 90–95 %, which means that for this use, with the endoscope terminal attached, the irradiance values will be around 3.88 to 35.70 mW/cm², a situation that requires longer treatment times.

The inclusion of the digital device allows for easy control of the system, accessible to any member of a medical or research team.

The compatibility study between the proposed source and the photosensitizers porphyrins, chlorins, bacteriochlorins, methylene blue, and rose bengal shows that the device is optimized for treatments with PpIX precursors, presents high compatibility with chlorins, and that, for the other compounds, at least one or more wavelengths emitted by the source coincide with the absorption peaks of these. Therefore, we can consider that the proposed device presents high compatibility with the various photosensitizers analyzed.

Compared to our proposed device, alternative light sources for target treatments, such as lasers, exhibit monochromatic radiation, incur high costs, and require technical support along with regular calibrations.

5. Conclusions

The results obtained with the initial prototype in the pilot studies offer encouraging outcomes.

The proposed photodynamic therapy device enables external treatments with irradiance values and spectrum adjusted to 150 mW/cm², and internal treatments through the fiber optic terminal with a maximum value of 35.70 mW/cm².

The proposed device is low-cost, easy to use, manufacture, adjust, improve, and customize, whether by changing the wavelength of one of the arrays, adding more emitters per arm, redesigning the lower enclosure and internal finish, or the endoscope terminal coupling system.

The device shows great potential for both medical use and research applications.

Table 3
Characterization of assembled prototype with the fiber optic terminal attached at 0.50 cm: spectrum peaks, absolute irradiance for a 100 % PWM cycle, and for a 50 % PWM cycle.

Color	Red	Red	Violet	Cyan	Infrared	Green
Peak [nm]	632	634	407	474	783	518
Absolute Irradiance [mW/cm²] PWM Cycle 100 %	3.88	5.51	8.20	6.72	7.52	5.57
Absolute Irradiance [mW/cm²] PWM Cycle 50 %	1.86	2.46	3.86	3.19	3.56	3.08

Note: 1.- The device with all LED arrays active, 35.70 (100 %)−17.13 (50 %) mW/cm². 2.- PWM Cycle 100 % The PWM delivers 100 % of the power to the end receivers. PWM Cycle 50 % The PWM delivers 50 % of the power to the end receivers.

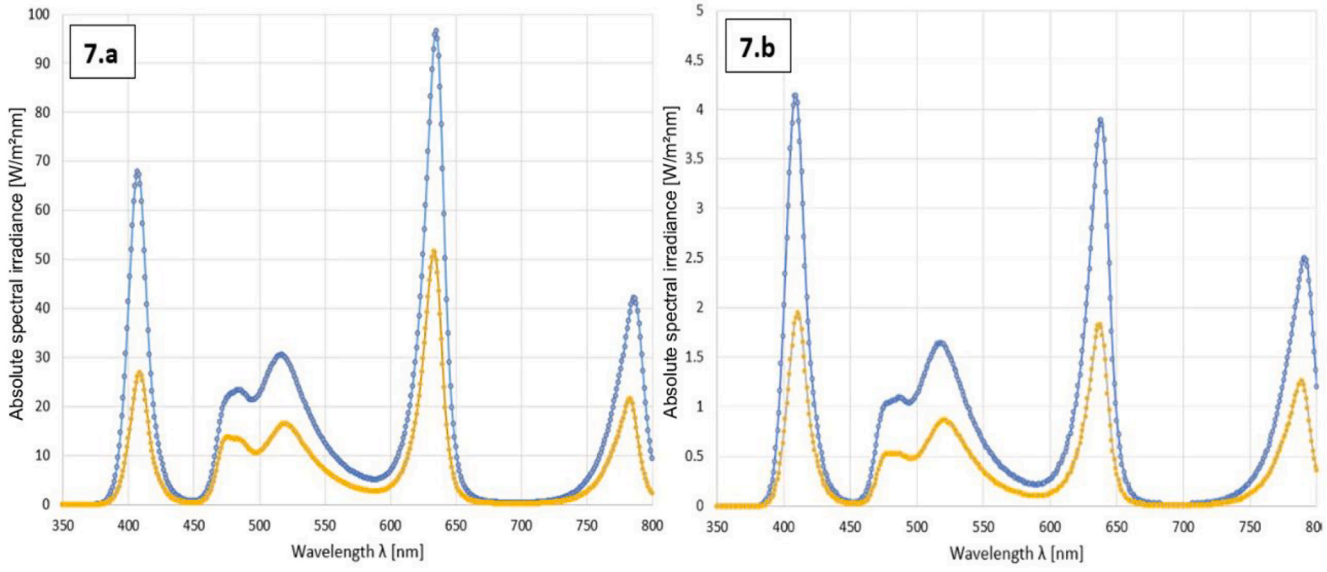

Fig. 7. Emission spectra of the device with all LED arrays activated at 100 % and 50 % irradiance. a.- WITHOUT fiber optic terminal endoscope coupling. b.- WITH fiber optic terminal endoscope coupling.

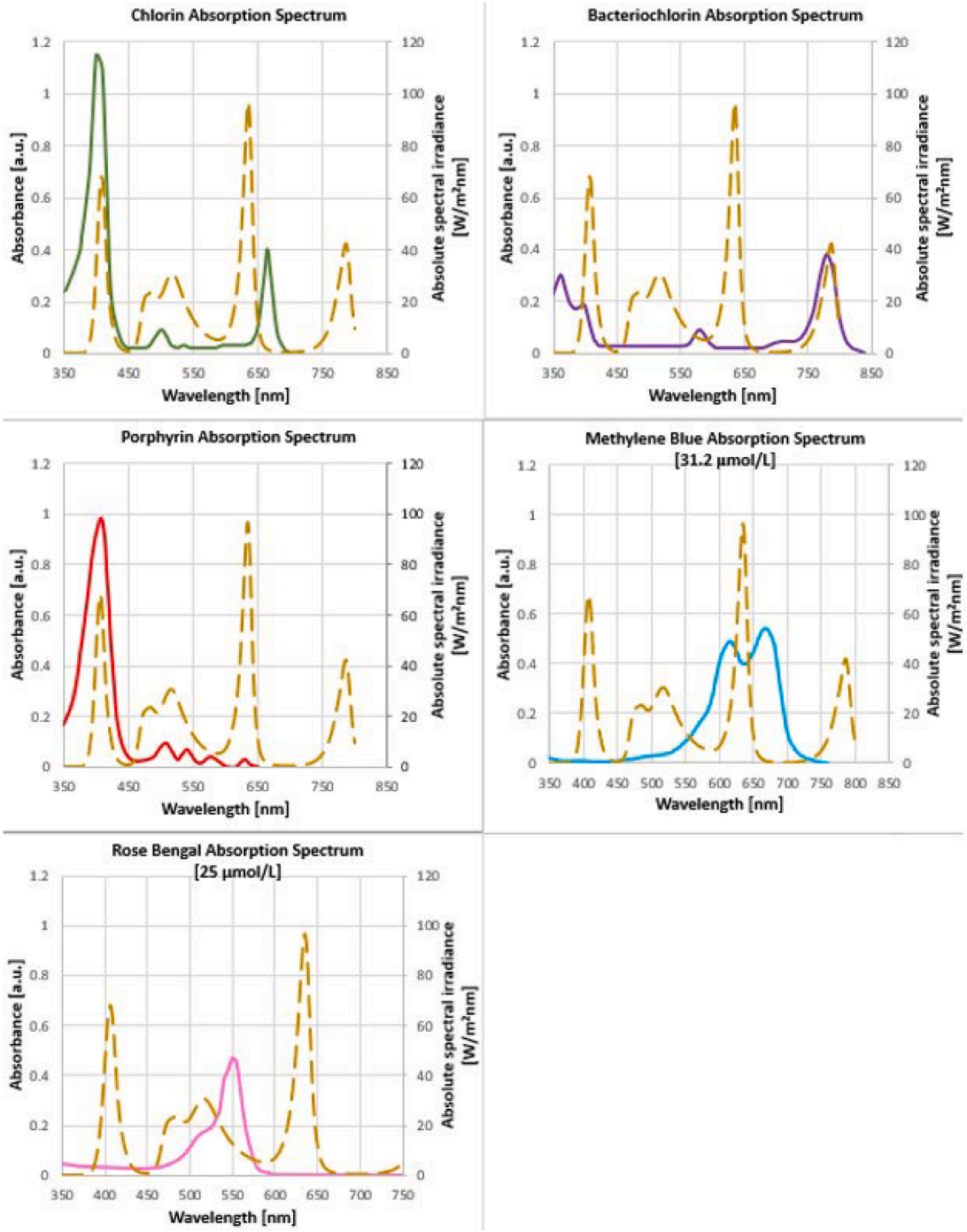

Fig. 8. Overlap of the absorption spectra of various photosensitizers commonly used in photodynamic therapy/research, and the emission spectrum of the source with all LED arrays connected. Solid line - photosensitizer absorption; dashed line - LED array emission.

CRediT authorship contribution statement

Enrique Navarrete de Gálvez: Writing – review & editing, Writing – original draft, Methodology, Funding acquisition, Formal analysis, Data curation, Conceptualization. **Pablo Fonda Pascual:** Supervision, Methodology, Formal analysis, Data curation. **José Aguilera Arjona:** Writing – review & editing, Supervision, Methodology, Data curation, Conceptualization. **José Ramón de Andrés Díaz:** Writing – review & editing, Supervision, Conceptualization. **María Navarrete de Gálvez:** Supervision, Investigation, Data curation. **Shiran Perera Mohamed:** Software, Methodology. **María Victoria de Gálvez Aranda:** Validation, Supervision, Methodology, Investigation, Formal analysis, Data curation.

Conflict of interest

The authors declare no competing interests.

Funding

This work has been supported by the project no. JA.B1-38-Junta de Andalucía's Own Plan Project. Project Reference: B1_2023-001. Project Organic: 08.09.20.33.28. Project Number: 00.941.075. And Universidad de Málaga/CBUA.

References

[1] S. Mordon, P.A. Martínez-Carpio, M. Vélez, R. Alves, Y.M.A. Trelles, «Terapia fotodinámica (PDT) en piel y estética: procedimiento, materiales y método en base a nuestra experiencia», Cir. Plást. Ibero-Latinoam. 38 (3) (2012) 287–295, https://doi.org/10.4321/S0376-78922012000300012, nsep.

[2] M. Panjehpour, B.F. Overholt, J.M. Haydek, «Light sources and delivery devices for photodynamic therapy in the gastrointestinal tract», Gastrointest. Endosc. Clin. N. Am. 10 (3) (2000) 513–532, https://doi.org/10.1016/S1052-5157(18)30120-X, njul.

[3] Y. Gilaberte, et al., «Terapia fotodinámica en dermatología», Act. Dermo-Sifiliogr. 97 (2) (2006) 83–102, https://doi.org/10.1016/S0001-7310(06)73359-2, nmar.

[4] C. Vicentini, J.-B. Tylcz, C. Maire, S. Mordon, Y.L. Mortier, «Terapia fotodinámica», EMC - Dermatol. 51 (3) (2017) 1–8, https://doi.org/10.1016/S1761-2896(17)85934-3, nsep.

[5] J.F. Algorri, M. Ochoa, P. Roldán-Varona, L. Rodríguez-Cobo, Y.J.M. López-Higuera, «Light technology for efficient and effective photodynamic therapy: a critical review», Cancers 13 (2021) https://doi.org/10.3390/cancers13143484 n14, Art. n. 14, ene.

[6] P. Robres, C. Aspiroz, A. Rezusta, Y.Y. Gilaberte, «Utilidad de la terapia fotodinámica en el manejo de la onicomicosis», Act. Dermo-Sifiliogr. 106 (2015) 795–805, https://doi.org/10.1016/j.ad.2015.08.005, n10dic.

[7] H. Abrahamse y, M.R. Hamblin, «New photosensitizers for photodynamic therapy», Biochem. J. 473 (4) (2016) 347–364, https://doi.org/10.1042/BJ20150942, nfeb.

[8] J.C. Kennedy, Y.R.H. Pottier, «New trends in photobiology: endogenous protoporphyrin IX, a clinically useful photosensitizer for photodynamic therapy», J. Photochem. Photobiol. B: Biol. 14 (4) (1992) 275–292, https://doi.org/10.1016/1011-1344(92)85108-7, njul.

[9] Photodynamic Therapy. Accedido: 26 de abril de 2024. [En línea]. Disponible en: https://link.springer.com/book/10.1007/978-1-0716-2099-1.

[10] R. Bonnett, «Photosensitizers of the porphyrin and phthalocyanine series for photodynamic therapy», Chem. Soc. Rev. 24 (1) (1995) 19, https://doi.org/10.1039/cs9952400019, n.

[11] M.H. Gold y, M.P. Goldman, «5-aminolevulinic acid photodynamic therapy: where we have been and where we are going», Dermatol. Surg. 30 (8) (2004) 1077–1084, https://doi.org/10.1111/j.1524-4725.2004.30331.x, nago.

[12] A.F. Taub, «5-aminolevulinic acid: acne vulgaris», in: M.H. Gold (Ed.), En *Photodynamic Therapy in Dermatology*, NY: Springer New York, New York, 2011, pp. 31–45, https://doi.org/10.1007/978-1-4419-1298-5_3.

[13] C.C.N. Sebrão, A.G. Bezerra, P.H.C. De França, L.E. Ferreira, Y.V.P.D. Westphalen, «Comparison of the efficiency of rose bengal and methylene blue as photosensitizers in photodynamic therapy techniques for *enterococcus faecalis* inactivation», Photomed. Laser Surg. 35 (2017) 18–23, https://doi.org/10.1089/pho.2015.3995, n1ene.

[14] L. Brancaleon y, H. Moseley, «Laser and non-laser light sources for photodynamic therapy», Lasers Med. Sci. 17 (3) (2002) 173–186, https://doi.org/10.1007/s101030200027, nago.

[15] C.A. Morton, C. Whitehurst, H. Moseley, J.V. Moore, Y.R.M. Mackie, «Development of an alternative light source to lasers for photodynamic therapy: 3. Clinical evaluation in the treatment of pre-malignant non-melanoma skin cancer», Laser Med. Sci. 10 (3) (1995) 165–171, https://doi.org/10.1007/BF02133327, nsep.

[16] S. Mordon, C. Cochrane, J.B. Tylcz, N. Betrouni, L. Mortier, Y.V. Koncar, «Light emitting fabric technologies for photodynamic therapy», Photodiagn. Photodyn. Ther. 12 (1) (2015) 1–8, https://doi.org/10.1016/j.pdpdt.2014.11.002, nmar.

[17] M.M. Kim, Y.A. Darafsheh, «Light sources and dosimetry techniques for photodynamic therapy», Photochem. Photobiol. 96 (2) (2020) 280–294, https://doi.org/10.1111/php.13219, n.

[18] S. Mallidi, S. Anbil, A.-L. Bulin, G. Obaid, M. Ichikawa, Y.T. Hasan, «Beyond the barriers of light penetration: strategies, perspectives and possibilities for photodynamic therapy», Theranostics 6 (13) (2016) 2458–2487, https://doi.org/10.7150/thno.16183, noct.

[19] C.A. Morton, et al., «Guidelines for topical photodynamic therapy: report of a workshop of the British Photodermatology Group», Br. J. Dermatol. 146 (4) (2002) 552–567, https://doi.org/10.1046/j.1365-2133.2002.04719.x, nabr.

[20] E.N. Gálvez, et al., «Analysis and evaluation of the operational characteristics of a new photodynamic therapy device», Photodiagn. Photodyn. Ther. 37 (2022) 102719 https://doi.org/10.1016/j.pdpdt.2022.102719 mar.